

Scanning interferometric method for measuring group delay of dispersive mirrors

Chengshuai Li (李承帅), Weidong Shen (沈伟东)*, Yueguang Zhang (章岳光),
Huanhuan Fan (范欢欢), and Xu Liu (刘旭)

State Key Laboratory of Modern Optical Instrumentation, Zhejiang University,
Hangzhou 310027, China

*Corresponding author: adongszju@hotmail.com

Received October 30, 2012; accepted December 12, 2012; posted online April 24, 2013

A scanning white-light interferometer is built for precisely measuring phase properties of dispersive multilayer thin film structure with the aid of the commercial spectrometer. Combining seeking optimal function for interferogram maximas with wavelet denoising algorithm, a novel time-domain algorithm is presented which enables the direct extraction of group delay and thus obtains a remarkable decrease of noise level in group delay and group delay dispersion. The apparatus shows reasonable potential for multilayer measurement, material characterization, displacement measurement as well as profilometry.

OCIS codes: 310.6845, 310.6188, 320.7090, 300.6300.

doi: 10.3788/COL201311.S10302.

With the development of commercial design software and ion assisted deposition, multilayer dispersive mirrors, such as Gires-Tournois (GT) mirrors or chirped mirrors, play a crucial role in ultra-fast laser system by providing precise dispersion compensation. Nevertheless, precise knowledge of its group delay (GD) as well as group delay dispersion (GDD), which are the first and second derivatives of the optical phase delay with respect to the angular frequency ω , respectively, though necessary for manufacturing and characterization of this device, is still a tough task. There are many different ways to approach for the measurement of these properties. Methods based on white-light interferometry (WLI), including the spectral method^[1] and temporal method^[2], are widely used for determination of the thin film structure reflection phase, as well as the GD and GDD. The spectrally resolved methods, often applying with Fourier transform^[3,4] or wavelet transform^[5], can retrieve the dispersion properties by a single measurement of the spectral interferogram intensity. However, limited by the small quantity and considerable noise of data acquired for one-shot spectral interferogram and the complexity derived from uncertainty of algorithm parameters^[6], it is difficult to extract precise GD or GDD information. For measuring of optical components directly, Knox *et al.*^[7] employed stepping motor and optical filter to get on the central wavelength of each filter, but the wavelength resolution was limited by the quality of optical filters. Beck *et al.*^[8,9] measured the changes in the optical path length (OPL) as a function of wavelength using He-Ne laser while the phase-locked interferometer was too complicated for operation.

In this letter, a novel scanning spectral interferometric method is presented for characterization of multilayer dispersive mirrors. By searching for the balance position on each interferogram corresponding to each wavelength and determining the accurate length the stepping motor moves for every step, we can figure out the phase changes brought by the reflection on dispersive mirrors

in the whole wavelength range.

A schematic of our scanning white-light spectral interferometer is presented in Fig. 1. It consists of a tungsten halogen lamp, a 50/50 home-made beam splitter made of BK7, input and output collimators, a Glan-Taylor prism polarizer which is employed to eliminate the interference in the beam splitter caused by s-component, two horizontal displacement platforms with test sample and reference mirror mounted on respectively, and a fiber-optic spectrometer with a spectral operation range from 350 to 1100 nm. The reference arm, with a high-reflection silver mirror on it, is driven by a stepping motor which varies the length of reference arm approximate linearly.

The white-light beam emitting from the tungsten halogen lamp is divided into two parts: one part reflected by the test sample, the other part reflected by the reference silver mirror. Both of the two parts are overlapped and collimated into the channel spectrometer. The spectral intensity distribution on every motor step is monitored and saved by the spectrometer,

$$I(\lambda, L) = I_0(\lambda) \left\{ 1 + V \cos \left[2\pi \frac{L}{\lambda} + \phi(\lambda) \right] \right\}, \quad (1)$$

where $I_0(\lambda)$ is reference spectrum, V is the envelope function of which the maximum appears when the total phase of the system is zero, L is the optical path difference between two arms in air, and $\phi(\lambda)$ stands for the phase changes on reflection of multilayer dispersive mirror we desire to know. Since the total phases of the system are determined by L and $\phi(\lambda)$, we can just trace the balance position, i.e., the position where the total phase of the system is zero and where the interferometric envelope function intensity is maximum.

We set the integrated time of the spectrometer as 8 ms and the average times as 5 to reduce the noise level in interference signal brought by vibration and CCD noise. Our stepping motor makes one step with 25–35 nm every 100 ms and we collect 6000 spectral scans which can almost cover the center range of dispersive region.

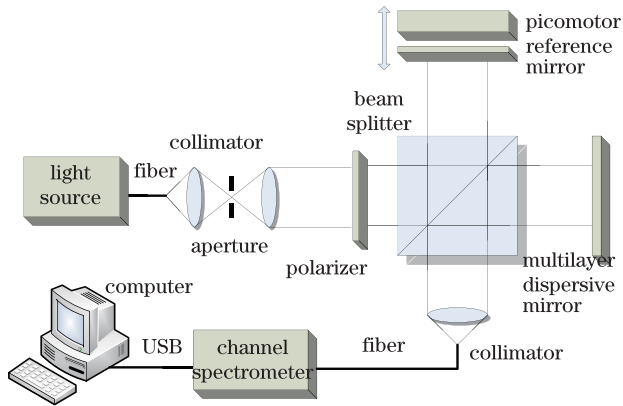


Fig. 1. Schematics of the scanning white-light spectral interferometer.

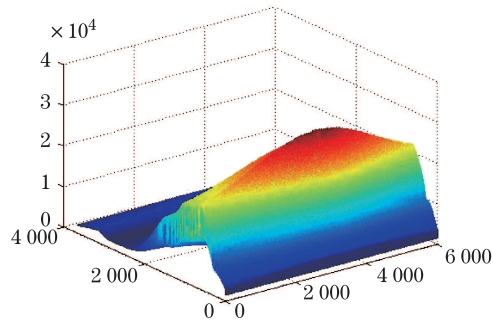


Fig. 2. Spectral intensity distribution recorded by spectrometer.

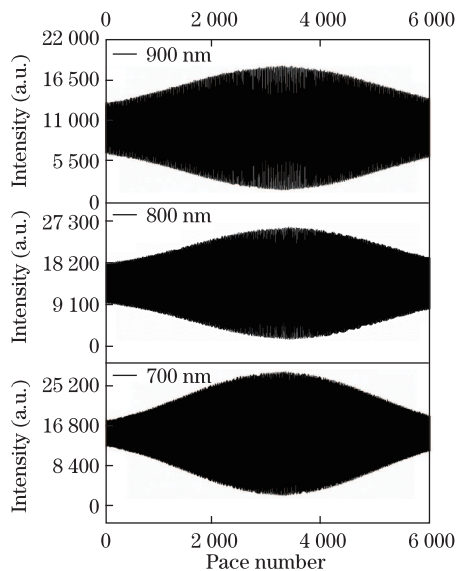


Fig. 3. Interferograms corresponding to different wavelengths.

One typical scanning interference signal recorded by the spectrometer is shown as Fig. 2.

Typical interferograms corresponding to different wavelengths are shown in Fig. 3. If there is no dispersive mirror on the sample arm, the balance position of each wavelength should be the same. If a dispersive mirror is mounted into the interferometer, then the balance positions of each wavelength will vary from each other because of the presence of phase shift on reflection

of dispersive mirrors. To find the balance position of each interferogram corresponding to different wavelengths, we first extract the positions of maximums and minimums in an interferogram using trigonometric function fitting. Thus the approximate outline curve of function V would be extracted from every interferogram (see Fig. 4).

In order to find the balance position of each interferogram, we apply the local extrema of the interferogram into Gaussian function with four parameters. By searching for the optimal solution of the parameters to describe the local extrema curve, we can get the Gaussian function which best describes the extrema of interferogram. Therefore, we can obtain the balance position from the parameters described in the form of pace numbers.

Note that the length of each step of the motor are not exactly the same, we should also calculate the exact pace length of the stepping motor. To get the relationship between L and pace number, we present a procedure for calculating length increments with every motor step. Consider the interferogram corresponding to one certain wavelength λ_n , as being shown in Fig. 5(a), measured intensity values can be easily found on a smaller segment marked by black dots in Fig. 5(b). The intensity is a trigonometric periodic function with the period of λ_n . Assuming that there are k paces in a semi period,

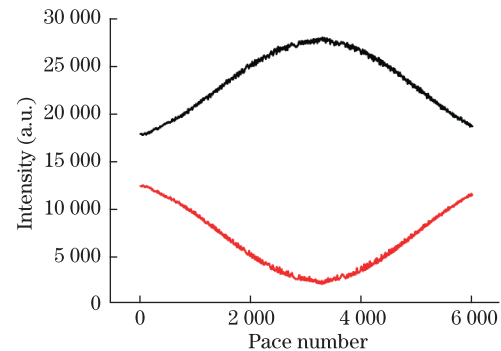


Fig. 4. Maximums and minimums of the interferogram corresponding to 700 nm.

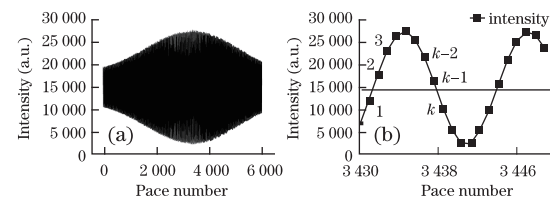


Fig. 5. Schematic illustrating the procedure of calculating pace length on each wavelength.

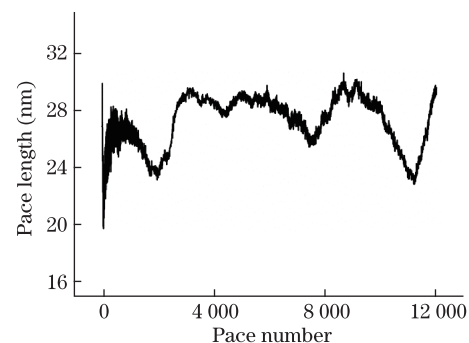


Fig. 6. Average pace length of every step.

then $I_1, I_2, I_3, \dots, I_{k-2}, I_{k-1}, I_k$ will be the intensity values achieved on each pace. If we make a simple assumption that every pace in one semi period is same, we can get the average pace length of this semi period,

$$l_n = \frac{\lambda/2}{(k-3) + \frac{I_2}{I_2-I_1} + \frac{I_{k-1}}{I_{k-1}-I_k}}. \quad (2)$$

Accordingly, we can get the groups of calculated pace length based on each interferogram corresponding to each wavelength. By averaging them, the exact pace length of every step can be acquired (see Fig. 6). Therefore, the balance position for each wavelength $L_b(\lambda)$ can be expressed by the optical length difference in the air. The corresponding GD and GDD of the dispersive mirror under test will be

$$\text{GD} = \frac{L_b(\lambda)}{c} + A, \quad (3)$$

$$\text{GDD} = \frac{\lambda^2}{2\pi c^2} \frac{dL_b(\lambda)}{d\lambda}. \quad (4)$$

Since the GD is extracted from the interferometric intensity data, the noise level of GDD will be much higher due to a straightforward numerical differentiation. For this reason, the denoising procedure is indispensable after the acquisition of GD. In our algorithm, we apply a method combing the cubic spline interpolation^[10] with wavelet denoising algorithm to reduce the noise level in GDD.

To certificate the feasibility and accuracy of our apparatus, the GDD properties of the home-made GT mirrors are measured. Two pieces of GT mirrors are designed to compensate GDD $\pm 400 \text{ fs}^2$ around 800 nm and manufactured by ion beam sputtering (IBS) simultaneously. After the procedure of seeking for balance position and

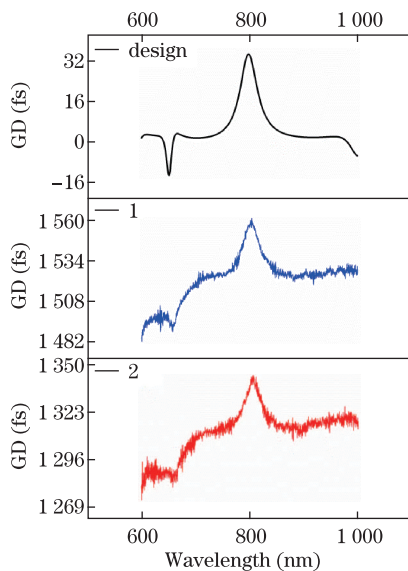


Fig. 7. Comparison of designed and measured GD curve of two GT mirrors.

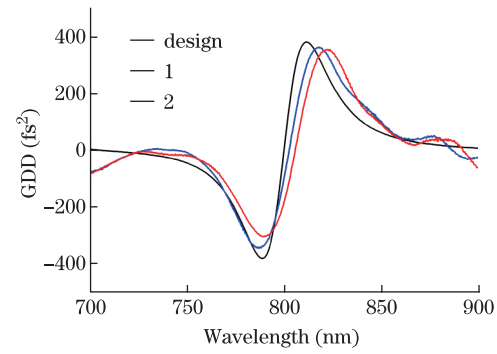


Fig. 8. (Color online) Comparison of designed and measured GDD curve of two GT mirrors.

calculating paced lengths, GD is acquired without denoising algorithm. Measured GD of the two GT mirrors in contrast with design one is shown in Fig. 7. The shape of measured GD curves is quite similar with the design one, especially around the central wavelength, regardless of the y -axis shift which is due to the uncertainty of parameter A in Eq. (3). The measured GDD of the two GT mirrors further verified our apparatus. The wavelength shift between measured and designed GDD is around 3 nm which is in the tolerance range of our manufacture procedure (see Fig. 8). In addition, the measured amplitude is a little smaller than designed GDD which may come from the denoising and smoothing algorithm.

In conclusion, a new method based on scanning interferometer for evaluating the GD and GDD of multilayer dispersive mirrors is proposed and experimentally demonstrated. It utilizes new algorithm for seeking for balance positions of interferograms and denoising method combing the cubic spline interpolation with wavelet denoising algorithm. Thus, the apparatus is a powerful tool for evaluating multilayer dispersive mirrors and a promising method which can expand to other application in thin film industry.

This work was supported by the National Natural Science Foundation of China (No. 61275161) and the Fundamental Research Funds for the Central Universities.

References

1. P. Hlubina, J. Lunacek, and D. Ciprian, *Opt. Lett.* **34**, 1564 (2009).
2. A. Gosteva, M. Haiml, R. Paschotta, and U. Keller, *J. Opt. Soc. Am. B* **22**, 1868 (2005).
3. P. Hlubina, J. Luňáček, D. Ciprian, and R. Chlebus, *Opt. Commun.* **281**, 2349 (2008).
4. H. Xue, W. Shen, P. Gu, Z. Luo, Y. Zhang, and X. Liu, *Chin. Opt. Lett.* **7**, 446 (2009).
5. Y. Deng, W. Yang, C. Zhou, X. Wang, J. Tao, W. Kong, and Z. Zhang, *Opt. Express* **17**, 6038 (2009).
6. Z. Luo, S. Zhang, W. Shen, C. Xia, Q. Ma, X. Liu, and Y. Zhang, *Appl. Opt.* **50**, C239 (2011).
7. W. H. Knox, N. M. Pearson, K. D. Li, and C. A. Hirli-mann, *Opt. Lett.* **13**, 574 (1988).
8. M. Beck and I. A. Walmsley, *Opt. Lett.* **15**, 492 (1990).
9. M. Beck, I. A. Walmsley, and J. D. Kafka, *IEEE J. Quant. Electron.* **27**, 2074 (1991).
10. C. H. Reinsch, *Numer. Math.* **10**, 177 (1967).